

Distinct center-of-mass quantization of light-hole and heavy-hole excitons in wide ZnTe-(Zn,Mg)Te quantum wells

Pierre Lefebvre and Vincent Calvo

Groupe d'Etude des Semiconducteurs, CNRS, Université Montpellier II, Case courrier 074, 34095 Montpellier Cedex 5, France

Noël Magnea

C.E.A. Grenoble, Département de Recherche Fondamentale sur la Matière Condensée/SP2M, 17, avenue des Martyrs, 38054 Grenoble, France

Thierry Taliercio, Jacques Allègre, and Henry Mathieu

Groupe d'Etude des Semiconducteurs, CNRS, Université Montpellier II, Case courrier 074, 34095 Montpellier Cedex 5, France
(Received 13 June 1997)

Samples consisting of a 36–38-nm-wide ZnTe quantum well with barriers made up of short-period ZnTe-MgTe superlattices were studied by low-temperature optical spectroscopy. The samples were grown by molecular-beam epitaxy on nominal (001) ZnTe surfaces. This structure allows the simultaneous observation of the quantization of the center-of-mass motion of both light-hole and heavy-hole excitons. The light- or heavy-hole characters are assigned by piezomodulated reflectivity experiments. The observed quantized energies are in reasonable agreement with the results of a simple model of an infinite quantum well, including “transition layers” near the well-barrier interfaces. This model cannot, however, account quantitatively for the observation of the fundamental resonances slightly below the transverse-exciton energy of bulk ZnTe. This effect is tentatively attributed to the strongly nonparabolic dispersion, in addition to more complex additional boundary conditions, for exciton polaritons with small wave vectors (approximately equal to twice the wave vector of light in the material). [S0163-1829(97)51140-4]

The recent interest in wide-gap semiconductors and in the development of high-quality nanostructures made from these materials, has opened up new possibilities for research on Wannier excitons and excitonic polaritons. In the *II-VI* materials, large excitonic binding energies and small Bohr radii allow observation of a variety of specific effects. For instance, one important consequence of these characteristics is the prominent role played by biexcitons in lasers based on wide-gap *II-VI* semiconductors.¹ Another consequence of small Bohr radii has been observed^{2–5} for wide *II-VI* semiconductor quantum wells, which are wider than ~ 2 Bohr diameters: the so-called center-of-mass quantization (CMQ), i.e., the quantum confinement of the excitonic polariton.

This particular confinement regime manifests itself by multiple resonances in optical spectra at energies which can be roughly described as the quantized levels of a particle in a one-dimensional quantum well, the relevant mass being the total excitonic effective mass. Comparable resonances of confined modes of the exciton polariton have been observed in submicronic high-purity ultrathin crystals of wurtzite CdS and CdSe (Ref. 6) and epilayers of zinc-blende GaAs.^{7–10} In wurtzite crystals, the upper valence bands are split apart by the crystal field so that the above-mentioned confined modes involve one single type of hole. For thin slabs of pure GaAs, evidence of this type of confinement was obtained only for heavy-hole excitons in Ref. 9, which the authors attributed to their larger oscillator strengths and density of states. Indirect indication of such an effect for light-hole excitons was obtained by comparison of optical spectra with theoretical calculations.^{8,10} In the extensive studies of Refs. 2–5, CdTe-(Cd,Zn)Te quantum wells with thicknesses between ~ 18 nm

and ~ 100 nm were investigated: due to the interplay of the valence-band offset and of lattice-mismatch strains, only electrons and heavy holes are confined in these CdTe layers. Consequently, the CMQ was only observed for heavy-hole excitons.

From the theoretical viewpoint, modeling the CMQ is made difficult by the combination of boundary conditions on electron and hole wave functions in quantum wells having different, finite depths, with the so-called additional boundary conditions (ABC),¹¹ which are necessary for treating excitonic polaritons. Models describing energies and amplitudes of the CMQ resonances have been developed, with various degrees of refinement, mainly depending on the particular system under consideration,^{7–14} but mostly in cases involving a single type of hole.

In this paper, we present results of low-temperature photoluminescence (PL) and reflectance spectroscopy, performed on two samples containing wide ZnTe quantum wells clad in barriers made of ZnTe/MgTe short-period superlattices. The samples were grown by molecular-beam epitaxy on (001)-oriented ZnTe substrates. The nominal width of the quantum wells is 120 monolayers (36 nm), i.e., at least 6 times the exciton Bohr radius in bulk ZnTe. Sample 1 is the bare ZnTe quantum well, while Sample 2 contains five equally spaced monomolecular inserts made of half monolayers of CdTe. These introduce trapped exciton levels at a few tens of meV below the excitonic gap of ZnTe. A detailed study, published elsewhere,¹⁵ demonstrates that these inserts tend to constitute a vertically ordered structure made of wide flat islands of CdTe, separated by wide clear spaces of ZnTe. The CMQ of both light-hole (lh) and heavy-hole

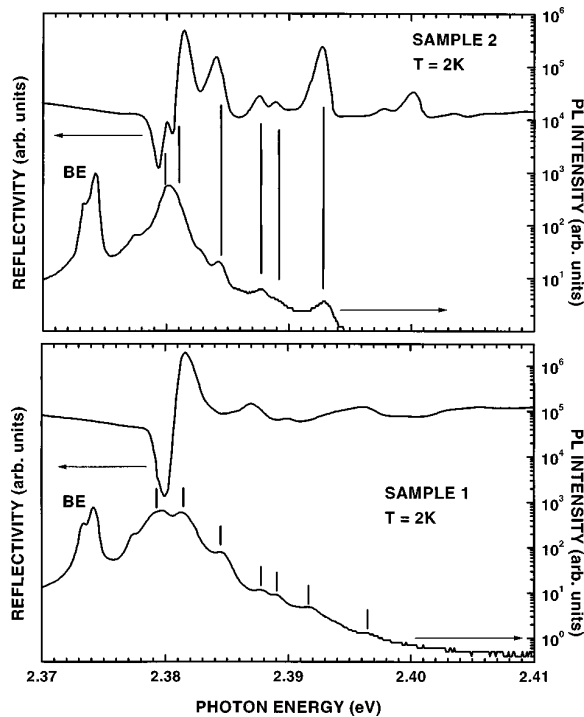


FIG. 1. Low-temperature reflectivity (linear scale) and photoluminescence (logarithmic scale) spectra of Samples 1 and 2. BE denotes impurity-bound excitons in the ZnTe substrates.

(hh) excitons can then take place across the whole ZnTe quantum well width through these clear spaces. For the purpose of the present work, the presence of CdTe islands will thus play no decisive role.

Continuous reflectivity and PL experiments were conducted with conventional setups: the samples were immersed in pumped liquid helium ($T \sim 2$ K) and illuminated either by an Ar^{++} laser (PL experiments) or by a 100 W tungsten lamp (reflectivity). The emitted or reflected light was dispersed by a HRS Jobin-Yvon spectrometer and detected by a photomultiplier in the standard way with lock-in detection. For piezomodulation experiments, a cold-finger cryostat with liquid He circulation, giving a sample temperature of ~ 10 K, was used; the samples were glued onto a piezoelectric transducer driven by an alternating voltage so as to undergo a small, alternating, in-plane biaxial strain. Differential spectra were obtained by detecting the signal variations synchronously with the driving voltage. This is known to provide a signal proportional to the first-order derivative of the direct optical spectrum, but with coefficients depending on the symmetry of the valence-band states (lh or hh) involved in the optical transition.^{16–18} Due to the particular values of deformation potentials and elastic constants in the present ZnTe-based structures, reflectance features involving light holes are modulated ~ 2.3 times more than those involving heavy holes. This supermodulation coefficient is less dramatic than the value of -16 reached by CdTe-based structures,^{17,18} but it surely yields the direct assignment of the observed transitions.

Figure 1 displays the cw PL and reflectance spectra of Samples 1 and 2, obtained at $T = 2$ K. The PL spectra are plotted on a logarithmic scale, in order to emphasize the weaker contributions. A system of reflectance oscillations

appears for both samples. Interference is likely to occur between the lowest resonances and the reflectance feature due to free excitons in the substrates of bulk ZnTe, which should be centered around ~ 2.381 eV. Luminescence from these bulk free excitons should be very weak. A very small bump in the PL spectra at 2.383 eV is attributed to Raman scattering of photons from the 514.5 nm laser line by ZnTe LO phonons (26.1 meV). At slightly lower energy (~ 2.373 , 2.374, and 2.377 eV), lie PL lines labeled BE assigned to bound excitons in the substrates, which are associated with no reflectivity feature. These assignments have been cross checked by direct PL measurements of the substrates, taken on the back of the samples, and are in agreement with previous studies of bulk ZnTe.¹⁹ Reflectance structures characteristic of hh and lh excitons in the barrier superlattices of Sample 1 (Sample 2) lie, respectively, at 2.43 and 2.445 eV (2.465 and 2.49 eV). Thus the “potential wells” which confine hh and lh excitons in Sample 1 (Sample 2) have depths of ~ 50 and 60 meV (80 and 110 meV), respectively. The difference between the two samples mainly arises from different compositions of the barrier superlattices.

Starting slightly below and extending well above the excitonic gap of bulk ZnTe, several reflectance and PL features appear for both samples. The reflectivity features are more visible in Sample 2 than in Sample 1, which we tentatively relate to the higher confinement potential. We assign these features to the first observation of CMQ resonances in ZnTe quantum wells. In first support of this assignment comes the observation of numerous excited states by PL, incompatible with a simple thermal population. The same effect had been observed in previous work on CdTe wide quantum wells² and explained by the difficult thermalization between the various CMQ states.

It is possible to distinguish between hh and lh excitons among these states by their strain sensitivities. Figure 2 presents a comparison of the piezomodulated reflectivity with the numerical derivative of the ordinary reflectivity spectrum. The temperature is close to ~ 10 K here and is not fully controlled so that the spectral features are slightly shifted to lower energies from their 2 K positions in Fig. 1. The amplitudes of both types of spectra have been matched onto each other for the fundamental heavy-hole transition of the barrier (not shown). Then, all cases of superpiezomodulation can be directly assigned to lh excitons and all cases of isomodulation to hh excitons. These assignments are explicitly shown in Fig. 2 by ℓ_i and h_j labels. Labels $h + \ell$ simply denote the accidental superimposition of hh and lh resonances; the assignment of h_4 and ℓ_3 resonances in Sample 2 was confirmed by reflectivity spectra taken at $T = 2$ K, where these transitions are more clearly resolved than for $T \sim 10$ K (see Fig. 1). For both samples, distinct PL peaks, shown by markers in Fig. 1, are only observed for transitions involving heavy holes, although a deconvolution procedure would probably reveal lh excitons as well. This allowed us to measure the energy of h_4 in Sample 1 and h_3 in Sample 2. The attribution of quantum numbers to the resonances was done by the fitting detailed in the next section.

We have tried to validate a simple model involving an effective quantum well with infinite potential barriers, which would mirror the actual system. To this extent, it is necessary to compare the measured resonance energies with the quan-

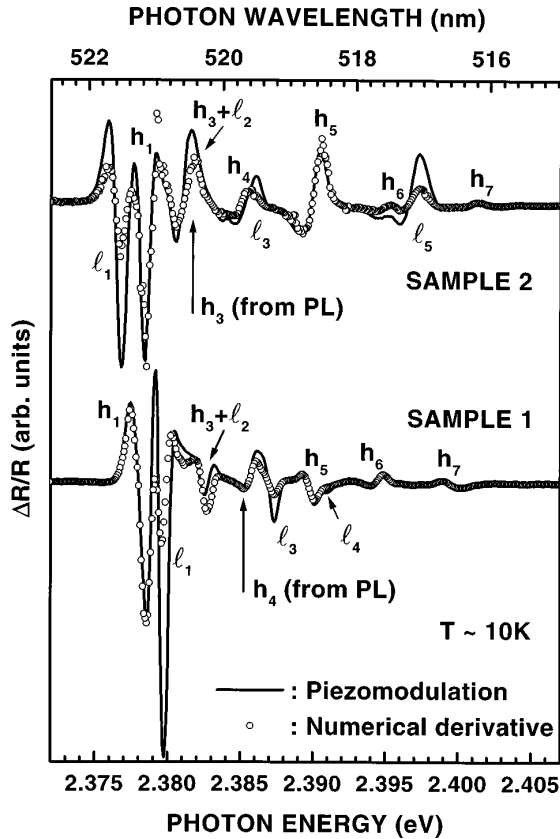


FIG. 2. Piezoreflectance (solid line) and numerical first derivative of the reflectivity spectra (open dots) of Samples 1 and 2, taken at ~ 10 K. These spectra have been scaled so as to be matched in amplitude for the heavy-hole exciton transition in the barrier superlattice (not shown). All lines where both spectra are closely matched are thus assigned to heavy holes (h); all resonances where the piezomodulation yields stronger features are assigned to light holes (ℓ).

tized polariton modes of a one-dimensional ideal well of effective thickness L_{eff} . For much larger layer thicknesses than in our samples, these modes would be selected from the spatial dispersion relation of the exciton polariton in ZnTe by the following simple rule: $k = N\pi/(L_{\text{eff}} - 2L_D)$ ($N=1,2, \dots$), where L_{eff} is an equivalent length and L_D the width of a dead layer or transition layer,^{11-14,20} accounting for the distortion of the center-of-mass motion near the layer surface. The value of L_D is comparable to the Bohr radius.

Here, the situation is complicated by several factors: first, the correct resonance wave vectors must be obtained by solving Eqs. (5) and (6) of Ref. 12, instead of the above simple rule because the layer width is not extremely large compared to the Bohr radius. These equations are

$$k_N \tan(k_N L_{\text{eff}}/2) + L_D^{-1} \tanh(L_{\text{eff}}/2L_D) = 0 \quad (1)$$

for $N=1,3,5, \dots$ and

$$k_N^{-1} \tan(k_N L_{\text{eff}}/2) - L_D \tanh(L_{\text{eff}}/2L_D) = 0 \quad (2)$$

for $N=2,4,6, \dots$.

Second, we need to include the two excitonlike polariton branches (lh and hh excitons) in zinc-blende materials.²¹⁻²³ The numerical parameters needed for this description (effec-

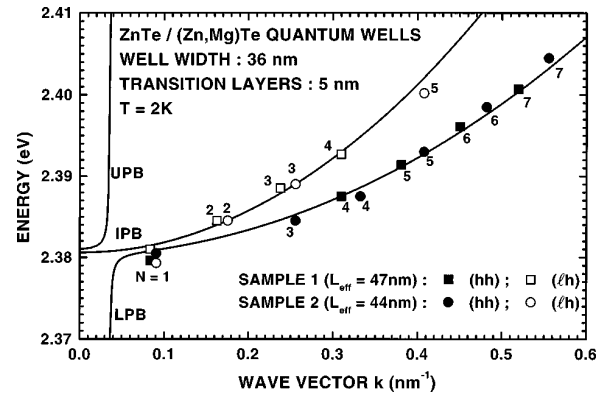


FIG. 3. Solid lines: the threefold spatial dispersion of exciton polaritons in bulk ZnTe (UPB, IPB, and LPB represent the upper, intermediate, and lower polariton branches, respectively). Dots: our best attempt at matching the present experimental hh- and lh-exciton resonances with the dispersion curves. The corresponding quantized k vectors have been obtained by solving Eqs. (1) and (2); the relevant quantization numbers are indicated near each experimental point.

tive masses, transverse-exciton energy, longitudinal-transverse splitting, k -linear term, \dots) need to be known with accuracy. Third, due to different reduced masses along the growth axis, the transition layers may not have the same thickness for lh and hh excitons. Indeed, due to the lifting of the valence-band degeneracy, lh excitons have a reduced mass along the (001) axis smaller than that of hh excitons, while the opposite is true for the in-plane reduced masses. The exciton envelope functions are then strongly anisotropic, with different pseudo-Bohr radii parallel and perpendicular to the quantization axis of the system.

Also, we should mention that, from the experimental viewpoint, it is never simple to extract the central resonance energy from reflectance spectra, especially in the present case where the resonances overlap with each other and with the substrate free exciton resonance. The last difficulty is that we are not totally sure that the MgTe and/or CdTe layers do not induce internal strains which may displace and change the anticrossing of lh and hh exciton polaritons.

Nevertheless, comparing our experimental results with the ideal slab model of Ref. 12, including typical dead layers $L_D=5$ nm, gives excellent fits, as displayed in Fig. 3. The material parameters used for the spatial dispersion calculations were taken or deduced from Ref. 24: electron mass, $m_e=0.166 m_0$; Luttinger parameters, $\gamma_1=4.07$, $\gamma_2=0.78$; relative static dielectric constant, $\epsilon_r=8.7$. The transverse-exciton-energy, $\hbar\omega_T=2380.6$ meV is an average value deduced from Refs. 19 and 24. A typical value of the longitudinal-transverse splitting, $\hbar\omega_{LT}=0.7$ meV has also been assumed. A satisfactory fit to experimental data for hh and lh polaritons has been obtained by using, respectively, the following effective widths: $L_{\text{eff}}=47$ nm for Sample 1 and $L_{\text{eff}}=44$ nm for Sample 2. These values have the correct order of magnitude since $(L_{\text{eff}} - 2L_D)$ is approximately the physical thickness of the ZnTe layer. As expected, the effective well widths are larger for Sample 1 than for Sample 2, which we attribute to the smaller potential discontinuity between the ZnTe well and the ZnTe/MgTe barrier superlattice, allowing for a deeper penetration of wave functions into the

barriers. A better fitting would probably be reached by including different dead layers for lh and hh excitons, which is not done here to avoid handling too many fitting parameters.

Concerning the amplitudes of CMQ resonances, it is known from previous studies on CdTe quantum wells²⁻⁵ that the resonances with different quantum numbers N obey particular selection rules, depending on the relative values of the well thickness and of the effective wavelength of light in the material. In ZnTe, the wavelength of photons is given by $\lambda_{\text{ph}} = \lambda_{\text{vacuum}}/n \sim 175$ nm, i.e., ~ 1.4 times smaller than in CdTe. In Ref. 2, a few rules derived from a simple model, involving ideal layers with thickness L and infinite potential barriers, were introduced. In later work, more sophisticated models for realistic systems have confirmed the predicted tendencies, which can be summarized as follows. For $L < \lambda_{\text{ph}}/4$, resonances with odd N have larger amplitudes than those with even N ; all resonances are of equivalent amplitude for $L = (2p - 1)\lambda_{\text{ph}}/4$, where $p = 1, 2, \dots$; confined polariton modes with odd N disappear for $L = (2p - 1)\lambda_{\text{ph}}/2$; modes with even N disappear for $L = p\lambda_{\text{ph}}$. For real structures with small discontinuities of the excitonic gap, these rules might not be strictly followed. In particular, the overall oscillator strengths are damped when going up to high quantum numbers.

Our samples, having 36-nm-thick wells, should both lie in the first category, since $\lambda_{\text{ph}}/4 \sim 44$ nm. Experimentally, the corresponding domination of resonances with odd N is indeed observed for both samples. However, this behavior is clearer for Sample 2 than for Sample 1. This is easily explained by the larger value of $(L_{\text{eff}} - 2L_D)$ for Sample 1, closer to $\lambda_{\text{ph}}/4$ than for Sample 2.

Next, it is important to notice that, although an overall good fit is obtained for the set of resonances, the fundamental resonances ℓ_1 and h_1 , for both samples, happen to lie at

a slightly lower energy than the value of $\hbar\omega_T$ assumed for ZnTe. Moreover, their ordering is different in the two samples. This second effect can be connected to the possibility of very small residual in-plane biaxial tension of the ZnTe layer provoked, in Sample 2, by the presence of MgTe and of CdTe inserts, which may put the ℓ_1 exciton at lower energy than h_1 . Now, concerning the absolute energies of these resonances in both samples, we remark that the resonance conditions taken from Ref. 12 may not be suitable in the present case of very small wave vectors, comparable to the wave vector of light in the material. We thus assign the present effect to the strong exciton-photon coupling (the polariton effect). Indeed, the latter should not only manifest itself in the spatial dispersion relation, but also through specific—more complex—boundary conditions. We thus believe that a more sophisticated theoretical description of the mixed system of lh and hh exciton-polariton resonances is necessary to account accurately for our data. Nevertheless, the assignment in terms of CMQ of lh and hh excitons is obviously correct.

We have presented the clear-cut observation of distinct quantization of the center-of-mass motion of light-hole and heavy-hole excitons in ZnTe/(Zn,Mg)Te quantum wells. In the domain of weak exciton-photon coupling, the corresponding resonance energies are in reasonable agreement with those of model ideal semiconductor slabs with adjustable effective widths and surface transition layers. In the region of strong polariton effect, this simple approach fails: the fundamental resonances lying slightly below the transverse-exciton energy of bulk ZnTe would be better accounted for by a refined model including specific boundary conditions. The latter would probably also yield a quantitatively correct modeling of the observed resonance amplitudes.

-
- ¹See, for example, F. Kreller, M. Lowisch, J. Puls, and F. Henneberger, *Phys. Rev. Lett.* **75**, 2420 (1995), and references therein; J. Ding, H. Jeon, T. Ishihara, M. Hagerott, V. Nurmikko, H. Luo, N. Samarth, and J. Furdyna, *ibid.* **69**, 1707 (1992), and references therein.
- ²H. Tuffigo, R. T. Cox, N. Magnea, Y. Merle d'Aubigné, and A. Million, *Phys. Rev. B* **37**, 4310 (1988).
- ³H. Tuffigo, in *Proceedings of Optics of Excitons in Confined Systems*, edited by A. D'Andrea, R. Del Sole, R. Girlanda, and A. Quattropani (Institute of Physics, Bristol, 1992), p. 37.
- ⁴H. Tuffigo, R. T. Cox, G. Lentz, N. Magnea, and H. Mariette, *J. Cryst. Growth* **101**, 778 (1990).
- ⁵N. Tomassini, A. D'Andrea, R. Del Sole, H. Tuffigo-Ulmer, and R. T. Cox, *Phys. Rev. B* **51**, 5005 (1995).
- ⁶See, for a review, E. L. Ivchenko in *Excitons*, edited by E. I. Rashba and M. D. Sturge (North-Holland, Amsterdam, 1982), pp. 159–162, and references therein.
- ⁷L. Schultheis and K. Ploog, *Phys. Rev. B* **29**, 7058 (1984).
- ⁸L. Schultheis, K. Köhler, and C. W. Tu, in *Excitons in Confined Systems* Vol. 25 of *Springer Proceedings in Physics*, edited by R. Del Sole, A. D'Andrea, and A. Lapicciarella (Springer-Verlag, Berlin, 1988), p. 110.
- ⁹A. Tredicucci, Y. Chen, F. Bassani, J. Massies, C. Deparis, and G. Neu, *Phys. Rev. B* **47**, 10 348 (1993).
- ¹⁰J. Kusano, G. E. W. Bauer, and Y. Aoyagi, *J. Appl. Phys.* **75**, 289 (1994).
- ¹¹K. Cho, A. D'Andrea, R. Del Sole, and H. Ishihara, *J. Phys. Soc. Jpn.* **59**, 1853 (1990), and references cited therein.
- ¹²A. D'Andrea and R. Del Sole, *Europhys. Lett.* **11**, 169 (1990).
- ¹³A. D'Andrea and R. Del Sole, *Phys. Rev. B* **41**, 1413 (1990).
- ¹⁴L. C. Andreani in *Confined Electrons and Photons*, Vol. 340 of *NATO Advanced Study Institute, Series B: Physics*, edited by E. Burstein and C. Weisbuch (Plenum, New York, 1995), pp. 57–112.
- ¹⁵P. Lefebvre, V. Calvo, N. Magnea, T. Taliercio, J. Allègre, and H. Mathieu (unpublished).
- ¹⁶H. Mathieu, P. Lefebvre, J. Allègre, B. Gil, and A. Regreny, *Phys. Rev. B* **36**, 6581 (1987).
- ¹⁷H. Mathieu, J. Allègre, and B. Gil, *Phys. Rev. B* **43**, 2218 (1991).
- ¹⁸V. Calvo, P. Lefebvre, J. Allègre, A. Bellabchara, H. Mathieu, Q. X. Zhao, and N. Magnea, *Phys. Rev. B* **53**, R16 164 (1996).
- ¹⁹N. Magnea, Thèse d'Etat (unpublished).
- ²⁰J. J. Hopfield and D. G. Thomas, *Phys. Rev.* **132**, 563 (1963).
- ²¹R. G. Ulbrich and G. Weisbuch, *Phys. Rev. Lett.* **38**, 865 (1977).
- ²²B. Sermage and G. Fishman, *Phys. Rev. Lett.* **43**, 1043 (1979); *Phys. Rev. B* **23**, 5107 (1981).
- ²³G. Fishman, *Solid State Commun.* **27**, 1097 (1978).
- ²⁴Ch. Neumann, A. Nöthe, and N. O. Lipari, *Phys. Rev. B* **37**, 922 (1988).